Journal of Theoretical and Applied Information Technology

31st August 2023. Vol.101. No 16

ISSN: 1992-8645 www.jatit.org E-ISSN: 1817-3195

CONSTRUCTION OF THE OPENING MECHANISM OF THE MIMOSA PUDICA BASED ON THE ANALYSIS OF VIDEO FRAMES FOR ARTIFICIAL LIFE IN CONFINEMENTS

JULIO CÉSAR BAUTISTA ROSAS [1], MARÍA FERNANDA GUILLEN PÉREZ[2], RODOLFO ROMERO-HERRERA[3]

[1]IPN, ESCOM, Department of Postgraduate, Ciudad de México

[2]IPN, ESCOM, Department of Postgraduate, Ciudad de México

[3]IPN, UPIITA, Department of Postgraduate, Ciudad de México

E-mail: jbautistar1500@egresado.ipn.mx[1], mariafernandagp23@gmail.com[2], rromeroh@ipn.mx[3]

ABSTRACT

The behavior of plants and trees, even when conducted unconsciously, we cannot ignore the fact that very useful algorithms can be obtained. In this project, mechanisms based on the movement and behavior of plants (mimosa pudica, Venus flytrap, toad, fruit trees, etc.) that can interact with humans were developed; for example, relieving stress situations when human beings are in states of confinement, such as the one experienced by the COVID-19 pandemic. This is because in many hospitals and closed places it is not feasible to introduce vegetation due to allergies or that the living system may be affected. In the project, digital image and video processing were applied to observe the movement of the plant. Key point detection techniques will be used for the digital processing of frames. With the data obtained, the behavior of the plant or tree is simulated for which the basic mechanics of the plant are built, and sensors are adapted. An additional advantage is that it requires a minimum of maintenance and has an impact on digital health. In the project, digital image and video processing were applied to observe the movement of the plant. For the digital processing of frames, key point detection techniques were used, a practice that, unlike other methods, simplifies the analysis and implements segmentation such as geodesy that are not used for this type of analysis, but that simplify the process and improve movement detection. With the data obtained, the behavior of the plant is simulated for which the basic mechanics of the plant are built, and sensors are incorporated to detect the environment surrounding the plant. An additional advantage is that it requires a minimum of maintenance and has an impact on digital health, with a mathematical model obtained through frames.

Keywords: *Mimosa Pudica, Behavior, Plants, Trees, Intelligence.*

1. INTRODUCTION

Nature-based systems have had a high boom, such as robots inspired by insects or animals, automaton mechanisms, and vision systems based on bird eyes, among many others [1][2]. Plants, for their part, have contributed a lot to medicine and other fields [3], so it is intended to understand how they work by discovering new ways of how they work internally [4]; however, despite their contributions, it is rare to find places where artificial life is used, even in those places where it is difficult to have natural vegetation.

Within the investigations that have been carried out on the behavior of plants, they have the ability to recognize their environment [5]; through electrical impulses that allows them to react through movements by collecting and translating their environment [6], they have a code similar to a neural network that allows them to coordinate their body organization by producing electricity; and they can be conceptualized as neurotransmitters as they are similar to a signaling molecule [7]. In such a way that it is possible with a previous study the generation of artificial plants that recognize their environment.

There are related works, one of them is the characterization of plant leaves employing Fisherse Vectors" [8], in which local descriptors calculated densely were used, with which they could identify the outline of the leaves without the need for a background. Visible, which allowed them to optimize the way leaves photographed in their natural environment were classified. Unlike the article [8], an analysis using digital image processing is presented, which simplifies the review.

There are various studies about the behavior of plants in which they are subjected to stress or pressure situations [9], where researchers look for the protection mechanisms of plants or how they adapt to new circumstances, which allows us to conclude the existence of a complex neurological system immersed in them or conjunction with various entities. When you observe them, they may seem like simple living beings, but the reality indicates the opposite since each leaf, stem, root, etc. It has sensors that allow us to imagine a brain planning strategies or processing information from the environment. [10] [11]. These sensors are implanted within the system that is proposed employing electronic circuits that allow detected vibrations or contact with the artificial.

The leaves of Mimosa pudica are categorized by the sleepy movement of their leaves at the slightest touch [12] [13]. The activity may be due to electrical signals and chemical components [14]. The movement can be divided into four stages: open, closed, blocked, and semi-open state [15] [16]. If there is an electrical component, it is a subject of investigation [17]; due to the possibility of a cyclic current-voltage signal, which if so would mean that plants have memory [18] [19]; So it is feasible to propose the mathematical and electrochemical representation of this fact [20]. However, these models are complex and therefore difficult to implement in artificial life, so it was proposed to emulate the 3 stages of movement using servomotors based on a previous analysis of frames taken from a video that detects the change in the position of the leaves.

In this paper, we review the movement of the mimosa pudica plant, which responds to the environment detecting presence by touch, temperature, and noise. The plant simulation design is based on electronic sensors so that hardware-based behavior can be obtained.

Observations of plants such as the Venus Fly Trap (Dionaea) or Sensitive Plant (Mimosa pudica) provide strong evidence that they can make the "muscles" of plants with stresses and forces. [21].

The technical challenge to develop is to design a plant variant that implements sensors that emulate the Mimosa pudica. The main importance lies in having a robot imitate intelligent behavior in plants and establish a link with mimosa pudica through mathematical models based on frames taken from videos.

The objective of this project is to find a methodology that allows detecting the movements made by plants based on changes in the segmented area of frames, by perceiving their environment (the situation before and after contact) and then mechanically simulating their behavior. It is proposed to use the Otsu method and the Geodesy method for segmentation. Classically, to analyze an object, segmentation by color is used, but this form of recognition generates errors, especially when considering the movement of an object [22].

2. METHODS AND MATERIALS

In the development of this work, the comportment of the Mimosa pudica plant, which presents the peculiarity of closing itself under environments of movement, touch, or temperature, was simulated. See Figure 1.

Figure 1: Mimosa pudica simple leaf.

2.1 Block diagram

For the study of the movement of the plant, a procedure was established that has the steps listed:

1. Obtaining frames.
2. Grayscale
3. Edge detection
4. Segmentation geodesy
5. Obtaining the area

The proposal for the mechanism is shown in Figure 2. The design considered a temperature sensor, a touch sensor, and an accelerometer. A Micro bit card, a servo, and the power supply were also considered.

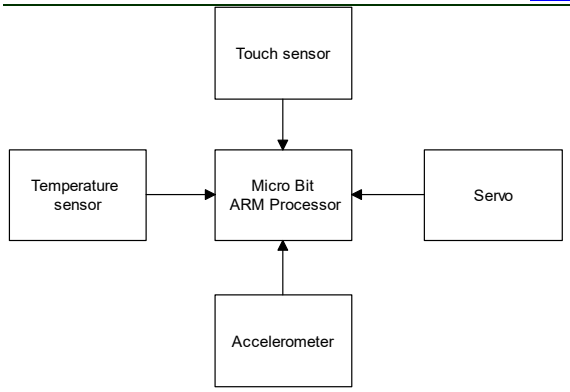

Figure 2: Checkered diagram, development proposal.

2.2.2 Procedure

The program recognizes the moments in which the plant has a change due to its movement; Two segmentation methods were programmed, and geodesy is the one that shows the best results. As input, there are videos of the plant and from here the frames are taken, to which the proposed segmentation is applied. The number of images taken depends on the length of the video; which varies the number of frames obtained; including frames containing letters, like many that exist on the internet [23]. In Figure 3, the first frame is shown; which reflects a time before contact. In Figure 4, you can see frame 78 of a public domain video [23], which occurs after the leaves touch, so it begins to close.

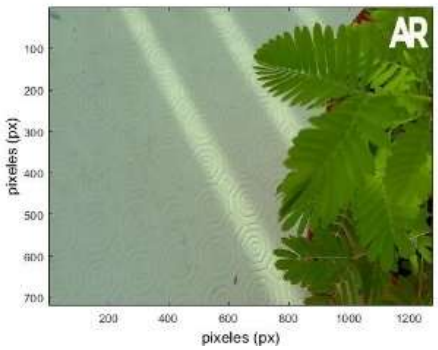

Figure 3: Frame number 1

Figure 4: Frame number 78 [23].

The analysis to detect a change was based on frames taken at time intervals considering thresholds. Figure 5 shows the diagram of the technique used. In the first step, a grayscale was applied to the frames (Figure 6), and the edges were detected (Figure 7), once these techniques were applied to the images, the image segmentation methods were applied. (Figure 8), and statistical parameters are obtained where the change in the area stands out, which allows us to determine that the plant has moved.

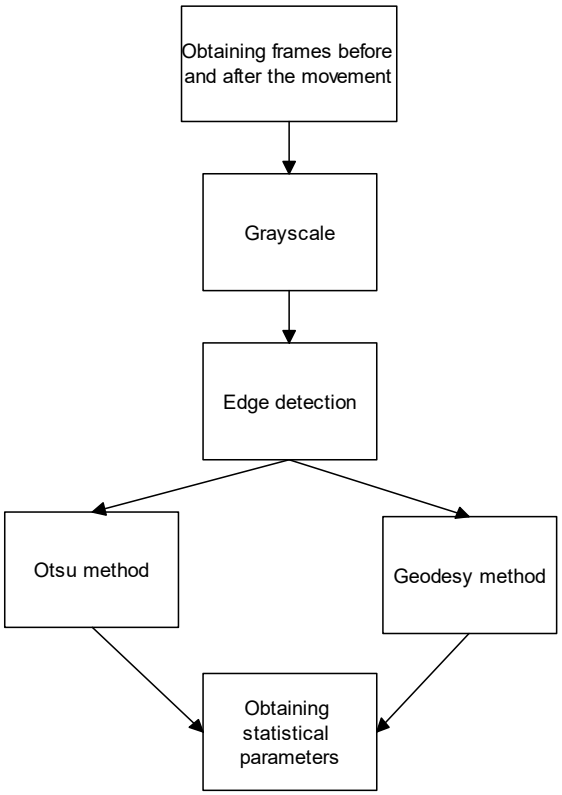

Figure 5: Block diagram of the procedure

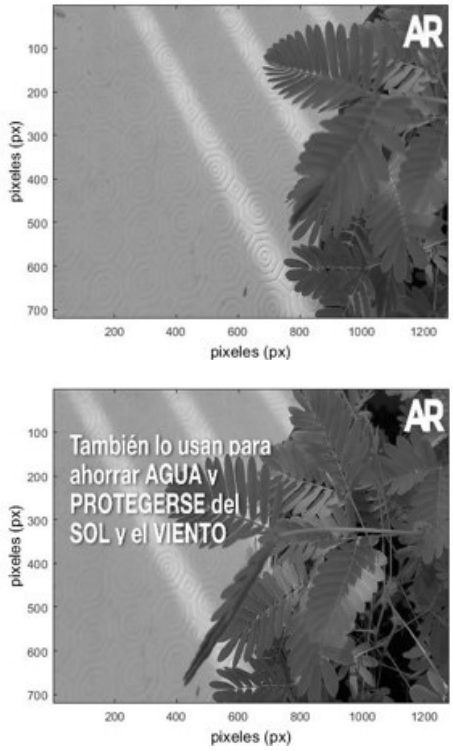

Figure 6: Grayscale frames.

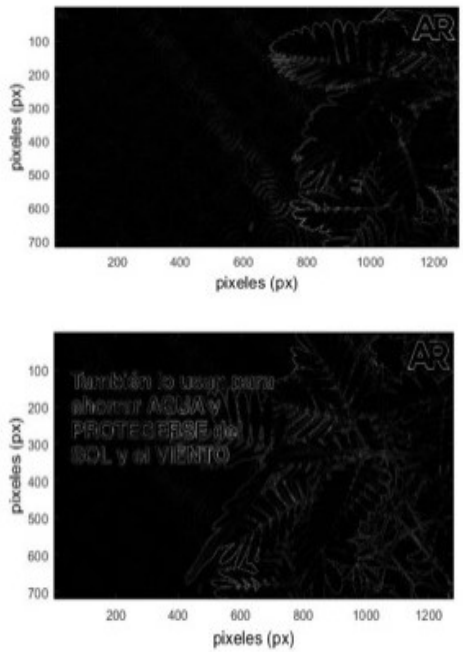

Figure 7: Frames with borders.

Figure 8. Difference of frames in pixels.

The program detects the moments in which the plant made some change, manifesting itself in movement [24].

2.2.3 Otsu Method

Two segmentation techniques were implemented to obtain the area. In the first program, the Otsu method was applied. This method consists of coloring the area of interest purple; It is a technique used when there is a considerable discrepancy between the background of the image and the object that we want to extract, this method is based on the similarity between the pixels [25]. Therefore, the image must contain similar objects and a background that contrasts them. Within our program, the application of the frame difference allows us to visualize the area of the movement of the plant in a clearer way concerning the background. The Otsu method uses a global threshold to transform an image to its binary equivalent, depending on the threshold, T; setting to '1' the pixels concerning the object and '0' to those belonging to the background. With the objective that the objects are clear to the background, the following is applied:

$$g(x,y) = \begin{cases} 1 & \leftrightarrow f(x,y) > T \\ 0 & \leftrightarrow f(x,y) \leq T \end{cases} \quad (1)$$

If the background is light and the object is dark, the mapping is reversed:

$$g(x,y) = \begin{cases} 1 & \leftrightarrow f(x,y) < T \\ 0 & \leftrightarrow f(x,y) \geq T \end{cases} \quad (2)$$

There are 3 types of threshold, the local one that depends on f (x, y), the global one that is a function of the local property of the pixel, p(x,y), and the dynamic one that depends on the location (x,y) of the pixel:

$$T = T(f(x,y), p(x,y), x, y) \quad (3)$$

Otsu method chooses the best threshold and makes the best use of the between-class variance through a

search that evaluates the threshold and thereby takes full advantage of the between-class variance [8]. As the classes of an image increase, the time increases due to the need to have multilevel thresholds [26]. The benefit of this technique is that it is automatic, therefore it does not require prior information on the image before processing.

An image is made up of N pixels whose gray levels are between 1 and L. In (4) the probability of occurrence is calculated where fi are of pixels with gray level i.

$$p_i = \frac{f_i}{N} \quad (4)$$

When the pixels are binarized, two classes are taken into account: C1, with gray levels [1, …, t]; and C2, and from [t+1, …, L]. So, for the two classes, the probability distribution is:

$$C_1 : \frac{P_1}{\omega_1}, \ldots, \frac{P_t}{\omega_1(t)} \quad (5)$$

$$C_2 : \frac{P_{t+1}}{\omega_2(t)}, \frac{P_{t+2}}{\omega_2(t)} \ldots, \frac{P_L}{\omega_2(t)} \quad (6)$$

Where:

$$\omega_1(t) = \sum_{t=1}^{t} P_i \quad (7)$$

The mean for class C1 and class C2 is:

$$\mu_1 = \sum_{i=1}^{t} \frac{i\, p_i}{\omega_1(t)} \qquad \mu_2(t) = \sum_{i=t+1}^{L} \frac{i\, p_i}{\omega_2(t)} \quad (8)$$

If μT is the average intensity of the image. It is easy to check that:

$$\omega_1 \mu_1 + \omega_2 \mu_2 = \mu_T \qquad \omega_1 + \omega_2 = 1 \quad (9)$$

Otsu defines the between-class variance using discriminant analysis using eq (10).

$$\sigma_B^2 = \omega_1(\mu_1 - \mu_T)^2 + \omega_2(\mu_1 - \mu_T)^2 \quad (10)$$

In the case of double-level Otsu, it is tested that the optimal threshold t* is such that σB2 is maximum:

$$t^* = {}^{Max}_{t}\{\sigma_B^2(t)\} \qquad 1 \le t \le L \quad (11)$$

To apply the Otsu method at multiple levels, M-1 thresholds must be considered, {t1, t2, ..., tM-1}, which divides the image into M classes:

- C1 in the case of [1, ..., t1]
- C2 in the case of [t1+1, ..., t2]
- Ci in the case of [ti-1+1, ..., ti]
- CM in the case of [tM-1,...,L]

To maximize σB2 the ideal thresholds {t1*, t2*, ..., tM-1*} are chosen as follows:

$$\{t_1^*, t_2^*, \ldots, t_{M-1}^* = {}^{Max}_{t_1, t_2, \ldots, t_{M-1}}\{\sigma_B^2(t_1, t_2, \ldots, t_{M-1})\}\} \quad 1 \le t_1 < \cdots < t_{M-1} < L \quad (12)$$

Where:

$$\sigma_B^2 = \sum_{k=1}^{M} \omega_k\, (\mu_k - \mu_T)^2 \quad (13)$$

With:

$$\omega_k = \sum_{i \epsilon C_k} p_i \qquad \mu_k = \sum_{i \epsilon C_k} \frac{i\, p_i}{\omega_k} \quad (14)$$

ωk is an accumulated moment of order zero of the k-th class Ck, and from (10) we have:

$$\mu(k) = \sum_{i \epsilon C_k} i\, p_i \quad (15)$$

Once executing the code, we can see how the Otsu method has already segmented the purple zone from the rest of the frame, leaving only the area of the frame difference (Figure 9).

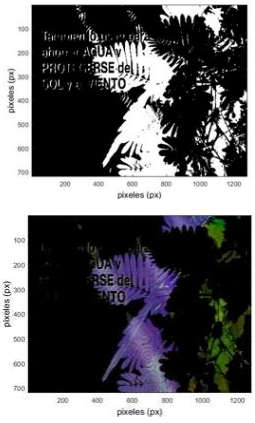

Figure 9: Otsu method applied to the frame difference.

2.2.4 Geodesia Method

The second technique used is Geodesy, which segments the image in colors, and binarizes it with labels that specify the location of the initial zones,

ISSN: 1992-8645 www.jatit.org E-ISSN: 1817-3195

the object to be analyzed, and the background, or in the case of being a color image with more region will return the image with trinary segmentation, with the labels in an array; these specify the location of the initial zones for the three regions.
In the article [27] [28] the basic idea of calculating conservation weights within a quadrangular window by using geodesic distances is stated. The geodesic distance D(p,c) among a pixel p in the sustenance window and the central window c is the minimum distance between p and c in the color volume [28].

$$D(p,c) = \min_{P \in P_{p,c}} d(P) \quad (16)$$

In the above equation Pp, c means the set of all pathways among p and c. A path P is demarcated as an arrangement of spatially neighboring points in 8-connectivity {p1, p2, ⋯, pn}. The dc () values of a route are computed by

$$d(P) \sum_{i=2}^{i=n} d_c(p_i, p_i - 1) \quad (17)$$

Where dc() is a method that defines the color difference. This function is calculated by:

$$d_c(p,q) = \sqrt{(r_p - r_q)^2 + (g_p - g_q)^2 + (b_p - b_q)^2} \quad (18)$$

where rp, gp, and bp are the RGB channel values of p.
Connectivity occurs if the geodesic distance from pixel p to the central window c is small because the connection between these points r varies only slightly in color.
Accept that pixels with low geodesic distance have an equal disparity as c. So little geodesic distances become high support weights. Equation (19) implements "w".

$$w(p,c) = \exp\left(-\frac{D(p,)c}{\gamma}\right) \quad (19)$$

γ is defined by the user and indicates the strength of the segmentation. When you have the weights, they are exploded to add pixel differences inside the window. The aggregate matching costs for a pixel c, at disparity d are resultant from:

$$m(c,d) = \sum_{p \in W_c} w(p,c)\, f(p, p-d) \quad (20)$$

With Wc in place of all pixels in the square window positioned on pixel c. The dimensions of the window are given by the user. The function f(p,q) determines the color difference between a pixel p of the reference image and an initial pixel q. The shared information is chosen in such a way as to allow the use of different lighting within two input images. An upper bound fmax is placed on the pixel difference to truncate values that exceed fmax; to reduce the effect of occluded pixels.
Por último, se determina un mapa de la disparidad dp de cada píxel p desde la vista de referenciada mediante una mejora local:

$$d_p = \underset{d \in D}{\operatorname{argmin}}\, m(p,d) \quad (21)$$

d is the set of all allowable disparities.

2.2.5 F. Description of the plant

The mimosa pudica is from America. It can be found in tropical areas [29]. Around 50 cm tall, it does not tolerate frost and its roots grow a lot.
The closing behavior is simulated in the system. The design of the plant falls on the mechanism of the node, the node is the base of a shoot, a leaf, and a twig. Even without visible buds or leaves, you can tell where the node is by a few visible signs. See Figure 10.

Figure 10: Mimosa points close, leaf open.

A sheet can be considered a structure of flat sheets. Most leaves can be shaped as thin membranes or sheets with vein and midrib reinforcements. The weak membrane folds due to the wind, which improves its resistance and blocks its destruction. But it is also required for the sheets to support their weight and other loads. Consequently, flexibility and

rigidity are important. The relations of these elements are what lead to an interesting mechanism. The leaves of the Mimosa pudica fold at different angles. The side view shows the way the sheets are folded. See Figure 11.

Figure 11: Mimosa pudica, lateral view.

To study the folds of the leaves in the veins, different factors were used. In Figure 5, Lo is the length of the unfolded sheet; Ho is the width of the unfolded sheet, LF is the length of the folded sheet; HF is the width of the folded sheet; α = vein angle; β= folding angle; X* = radial distance; Ao = unfolded area of the sheet; AF = folded area of the sheet.

The angle of the vein α, is the angle of deployment between the midrib and the vein; the folding angle β is the angle between the midrib and the vein when it is folded; Figure 12 shows the location of the veins X, dignified from the limit between the petiole and the leaflets. A non-dimensional parameter, X* defined as X* =X/Lo, was used to characterize the position of the ribs. The veins transport water and nutrients within the leaf and provide support, which defines its structure.

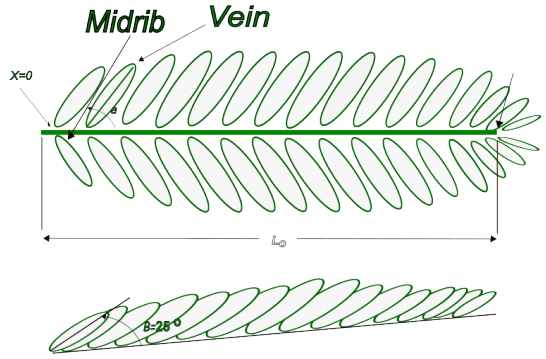

Figure 12: Schematic diagram of leaf dimensions together with vein angle (a) and fold angle (B).

2.2.6 Movement mechanism simulation

To simulate the movement of the leaves, various measurements were made based on programs for the segmentation of frames, to obtain the Variation X* versus the angle of the vein. The units can be considered dimensionless since we only want to obtain the equation that governs the dependency. Figure 13 shows this relationship.

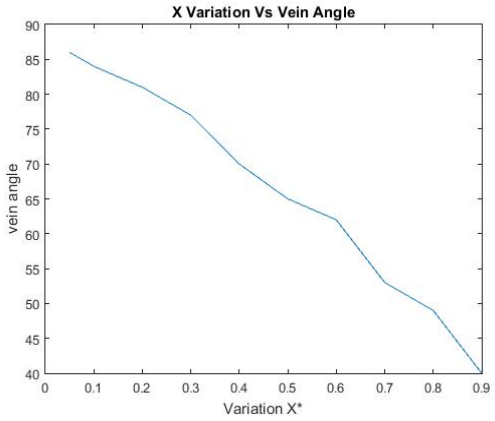

Figure 13: Graph X vs angle of the vein.*

The equations that govern the sleep movement of the Mimosa pudica were obtained to implement it in the microprocessor and simulate the folding of the leaves. The first is quadratic (22) and the second is the cubic representation of (23):

$$Angulo\ de\ la\ vena = 22.26X^{*^2} - 32.34X^{*} + 87.76 \quad (22)$$

$$Angulo\ de\ la\ vena = -2.883X^{*^3} - 18.17X^{*^2} + 87.88 \quad (23)$$

To simulate the deployment of a regular single leaf, a mechanism was designed (see Figure 9). The l model is useful for finding the folded and unfolded areas of the sheet. The folded area can be designed by folding the model simulation sheets at a particular constant angle (15º to 25º). This angle is represented as angle β. The area is measured by projecting the folded sheet onto aluminum foil and then cutting it. Five patterns of the variable folding angle of 15º, 17º, 20º, 22º, and 25º were considered to study the area proportions. To simplify the design, it was decided to only place 4 ribs. See Figure 14.

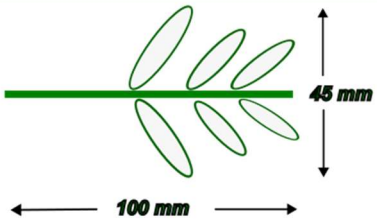

Figure 14: The leaf model with dimensions scaled like the original leaf.

Some rules in the simulation model must be taken into account:
1. Folding and unfolding are equal for the midrib.
2. The folding is even, and the folding angle is equal for all the flakes.
3. Folds do not store elastic tension energy.
4. The leaflets are flat rigid bodies, there is no alteration during unfolding.
5. Dimensions of the sheet are constant when folding and unfolding.
6. The total of pairs of leaflets on each leaf remains constant.

The folding of the structure is analogous to that of a Mimosa leaf. Nevertheless, due to the margins of the angular folds assumed to be the aluminum structure, there was a variance in the fold. In the real blade, the blade is twisted continuously at a certain angle (15º to 25º). As the folding angle β decreases from 25° to 15°, the folded area is compact.
To determine the result of the variances in the fold angle on the fold shape, two models of the paper structure were analyzed. The distance of the central rib of both models was 100 mm. Figure 15 is the main mechanism in its simulated version, which contains the mechanism that causes the movement.

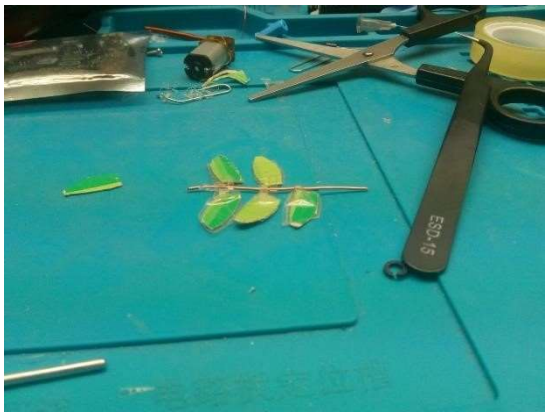

Figure 15: Mechanism test, leaf movement.

Figure 16 shows the robotic mechanism and the natural one of the plants. In this case, the node is the key to carry out the movement. To fold the sole, a screw is used, which rotates to convert the rotational movement to a linear one, which, being attached to the leaves of the mechanism, causes the fold.

Figure 16: Design comparison.

The connections of interest are presented in the diagram of Figure 17. To control the movement, a 4 x 5 cm Microbit embedded card was used that contains an accelerometer, a magnetometer, a compass, etc. So, it can be considered an IMU (Inertial Measurement Unit). It also has an ARM processor that allows us to program the servomotor, depending on what is sensed. For the program implemented in the Microbit, either equation (1) or (2) can be considered.

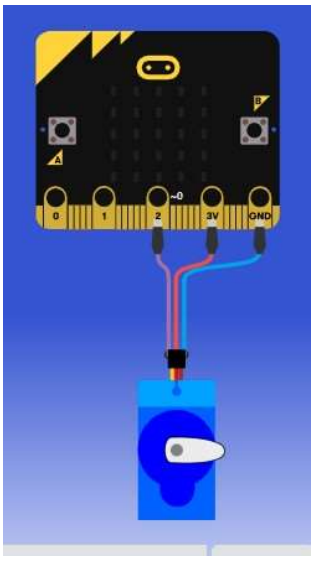

Figure 17: Microbit servomotor connection scheme

Figure 18 shows the temperature and touch sensors, with which it is possible to explore the functioning of the mimosa pudica plant and how it responds to its environment.

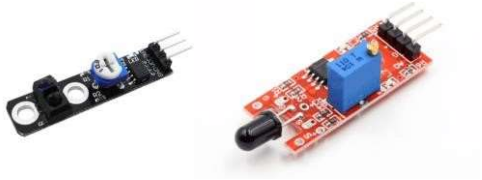

Figure 18: Flame detection sensors and touch detectors.

3. RESULTS

Once the methodology has been executed, we will be able to visualize how the Geodesy method generates the violet zone at the bottom of our frame, leaving only the area of the difference. In Figure 19 the letters have completely disappeared.

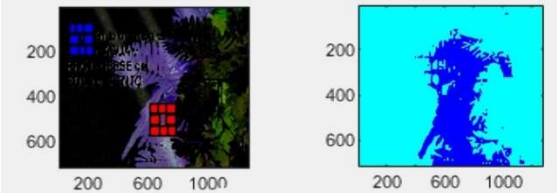

Figure 19: Geodesy method applied to the difference of frames in pixels.

When the two segmentation methods have been executed, the area of the difference between frames is calculated, with which the surface covered by the leaves of the plant is obtained when changing position; the area results were enclosed in a box to improve visualization within the Otsu method (Figure 20) and the Geodesy method (Figure 21). The numerical results were given by the command window of the program and later registered.

Figure 20. The area obtained in the Otsu method.

Figure 21: Area obtained in the Otsu method.

Graphs were made with the data obtained from the area, figure 10 and 11 it is shown what happens when touching the plant, changes that generate peaks in the graph are observed, and with this, the values obtained with the Otsu method are compared (Figure 22) and the Geodesy method (Figure 23).

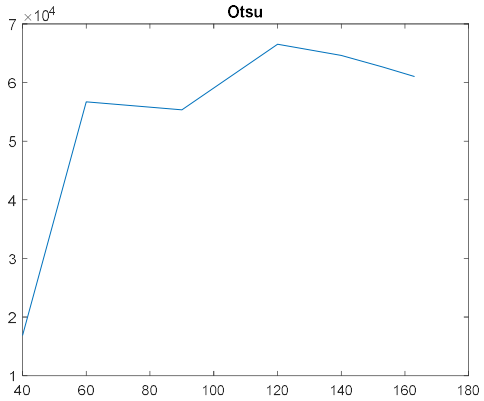

Figure 22: Graph of the area obtained in the Otsu method.

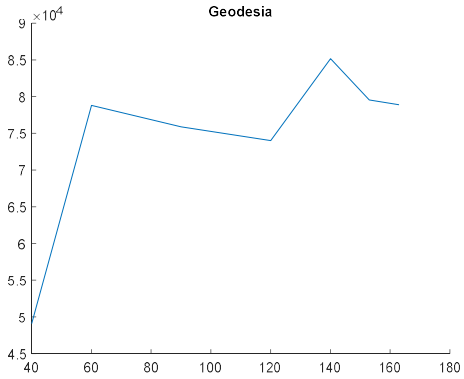

Figure 23: Graph of the area obtained in the Geodesy method.

The angle of the vein of the Mimosa pudica is not the same, slowly reducing from about 85º to 25º to the tip of the leaf. The average angle of the vein is around 55º.

Unlike the work of Fisher [8] where a product capable of detecting and classifying the type of plant leaf was obtained, the results obtained during the project were more focused on detecting movement from frames than plant leaves produced, for data recording. It should be considered that

finally beyond the analysis of a single image, it was possible to analyze a video.

Figure 24 shows the fold of the leaves of the plant. The main difference concerning the real model lies in the folding, although it is very similar, it presents margins of the angular folds of the aluminum model. As mentioned in the previous section, the real blade twists continuously at a certain angle (15º to 25º). As the folding angle β reduced from 25° to 15°, the folded area is compact. The aluminum model allows to model the angular behavior and vary its speed, to resemble its real counterpart.

Figure 24. Mimosa pudica closed leaf.

The closing of the leaves can be abrupt, so to avoid it, equation (22) was implemented in the Microbit card, although it is also feasible to use (23). Figure 25 is the control using a servo motor to achieve a subtle movement and keep the leaf open. Therefore, it fulfills the function for which it was designed. Figure 26 shows the complete system, the reason why they were made of aluminum was to preserve conductivity in them and allow simulation of the response to the touch of the real plant.

Figure 25: Mimosa pudica leaf open.

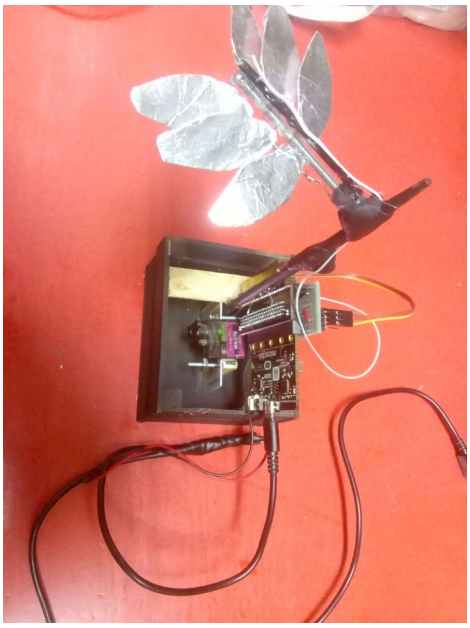

Figure 26: Implementation of connection of sensors to Microbit.

5. COMPARISON WITH RESPECT TO RELATED WORKS, PROS AND CONS

Unlike Volkov Alexander who proposes Fisher vectors [8] or the one proposed in [20] for the mathematical model of mimosa pudica, we apply digital image and video processing to analyze the movement of the plant and from there generate a simple mathematical model. Frames were used for the study, without stressing the plant; since they are video frames that occur when a change in the area is detected, see article [9]. Segmentation by color is not used, since the conditions do not allow detecting the leaves as there are more plants with similar characteristics in the background, as would normally be done [30]. A mathematical model based on movement was obtained, with which the artificial plant is built, to which sensors are incorporated to detect the environment that surrounds the plant; that is, it is susceptible to temperature changes,

vibrations, etc; which gives it a more real look. Giving the advantage of having a minimum of maintenance with an impact on digital health, since it is feasible to have it in hospitals where a natural plant can cause allergy problems.

Future work

Despite the advantages of the system, it has the disadvantage of having few leaves, so in the future, a system with greater characteristics is proposed, that is, more leaves and branches and even roots.

On the other hand, the artificial plant is not aware of the context, so it is proposed to develop a neural network system based on Transformers [31].

6. CONCLUSIONS AND IMPACT OF THE INVESTIGATION

It is of interest to obtain new mechanisms that allow understanding of the environment, trying to create new solutions that implement simulations of the behavior of nature. In our case, developing models that integrate the natural functioning of the mimosa pudica plant. Hardware-based systems allow the implementation of nature algorithm behaviors applied to artificial intelligence that interacts with the environment.

The analysis of the structure and folding form of the leaves of Mimosa pudica exposes some of the unusual characteristics through folding and unfolding. With this, it was possible to obtain equations to simulate the behavior of the movement of the plant's sleep and with it to develop prototypes with future applications. The mathematical models are simple to implement, unlike the proposal of the article Volkov.

The results allow us to interpret the behavior of the plants within an Artificial Intelligence model based on neurons, from a Graphic Interface where the methods of image segmentation and the calculation of the area due to the difference of frames in a video are applied. With whose data we can make prototypes to understand and apply the knowledge acquired, in the design of algorithms based on the behavior of plants.

Within the program, we were able to compare and observe the efficiency of two methods, where Geodesy was more suitable for image analysis and obtaining its area. Segmentation by color is not used when having plants as a background, as is commonly done; however, either technique is advantageous when compared to color targeting.

With the results, equations are obtained that can be prototypes to imitate the movement of the plant in question, and thus have a machine that is capable of making movements with a minimum of information regarding its environment, or in the specific case of the mimosa being able to detect your movement.

It was observed that the movement of the plant presents a behavior like a neural network in the transmission of movement. Which were simple to implement within the design, unlike the proposals.

Finally, since there is the intelligence of materials and other types of intelligence, it is not important to point out the existence of intelligence in plants. This type of project can help us determine a hypothesis in this regard. Since a functional system was achieved, the design of a network of robots to simulate neural behavior is proposed as future work.

7. ACKNOWLEDGMENTS

The authors thank the IPN (Instituto Politécnico Nacional) for the support received to carry out this project.

REFERENCES:

[1] Duran, Ricardo Rincón; Vega, Jorge Armando Niño; Morales, Flavio Humberto Fernández. Robot hexápodo para la enseñanza de mecanismos para la transformación de movimientos.*Revista Interamericana de Investigación Educación y Pedagogía RIIEP*, 2021, vol. 14, no 1, p. 279-303.

[2] Lopez Ramos, Carlos Alfredo Diseño y construcción de un Animatronic. 2017.

[3] Santillán, María Pilar Ruíz; Coico, Freddy Rogger Mejía. Plantas utilizadas en medicina tradicional para afecciones respiratorias virales. *Rebiol*, 2020, vol. 40, no 1, p. 109-130.

[4] Patil, H. S.; Vaijapurkar, Siddharth. Study of the geometry and folding pattern of leaves of Mimosa pudica, *Journal of Bionic Engineering*, 2007, vol. 4, no 1, p. 19-23.

[5] Basir, Siti Nora, et al. design concept of a new bio-inspired tactile sensor based on main pulvinus motor organ cells distribution of Mimosa Pudica plant. *International Symposium on Micro-NanoMechatronics and Human Science (MHS)*. IEEE, 2014. p. 1-6.

[6] Volkov, Alexander G., et al. Mimosa pudica: electrical and mechanical stimulation of plant movements. *Plant, cell & environment*, 2010, vol. 33, no 2, p. 163-173.

[7] Volkov, Alexander G. Signaling in electrical networks of the Venus flytrap (Dionaea muscipula Ellis). *Bioelectrochemistry*, 2019, vol. 125, p. 25-32.

[8] Redolfi Javier, Jorge A. Sánchez & Julián A. Pucheta, "Identificación de hojas de plantas usando Vectores de Fisher", ASAI, 16° *Simposio Argentino de Inteligencia Artificial*, [1]Centro de Investigación en Informática para la Ingeniería, Universidad Tecnológica Nacional, Facultad Regional Cárdoba, Maestro López S/N, [2]Universidad Nacional de Cordoba, Haya de la Torre S/N, [3]CONICET, Haya de la Torre S/N, (Cárdoba, Argentina), pág 3, 2015.

[9] Frantisˇek Balusˇka & Stefano Mancuso, " Plant neurobiology: from sensory biology, via plant communication, to social plant behavior", Marta Olivetti Belardinelli, *Springer-Verlag* 2008, págs. 1- 4, 8 November 2008.

[10] B. H. M. Appel & R. B. Cocroft, " Plants respond to leaf vibrations caused by insect herbivore chewing.", The Author(s) 2014, págs. 1-9, 2 July 2014,

[11] Quentin Hiernaux, " History and epistemology of plant behaviour: a pluralistic view?" *Springer Nature B.V*., págs. 1-624, June 2019.

[12] Wang, Yifeng; LI, Hua. Bio-chemo-electro-mechanical modelling of the rapid movement of Mimosa pudica. *Bioelectrochemistry*, 2020, vol. 134, p. 107533.

[13]Stolarz, Maria; Trębacz, Kazimierz. Spontaneous rapid leaf movements and action potentials in Mimosa pudica *L. Physiologia Plantarum*, 2021, vol. 173, no 4, p. 1882-1888.

[14] Pereira Gomes, Ayala Nara, et al. Chemical composition and free radical-scavenging activities of monofloral bee pollen from Mimosa pudica *L.Journal of Apicultural Research*, 2022, p. 1-8.

[15] A. G. Volkov et al, "Complete hunting cycle of Dionaea muscipula: Consecutive steps and their electrical properties," *Journal of Plant Physiology*, vol. 168, (2), pp. 109-120, 2011.

[16] Romero-Herrera, Rodolfo; Mendez-Segundo, Laura. Video Processing for Animation at Key Points of Movement in the Mimosa Pudica. *Iternational Journal of Advanced Computer Science and Applications*, 2020, vol. 11, no 9.

[17] Aishan, Yusufu, et al. Bio-actuated microvalve in microfluidics using sensing and actuating function of Mimosa pudica. *Scientific Reports*, 2022, vol. 12, no 1, p. 1-11.

[18] Biegler, Robert. Insufficient evidence for habituation in Mimosa pudica. Response to Gagliano et al.(2014). *Oecologia*, 2018, vol. 186, no 1, p. 33-35.

[19] Serpell, Ella; Chaves-Campos, Johel. Memory and habituation to harmful and non-harmful stimuli in a field population of the sensitive plant, Mimosa pudica. *Journal of Tropical Ecology*, 2022, vol. 38, no 2, p. 89-98.

[20] Kwan, K. W., et al. A Mathematical Model on Water Redistribution Mechanism of the Seismonastic Movement of Mimosa Pudica. *Biophysical journal*, 2013, vol. 105, no 1, p. 266-275.

[21] Tran, Daniel, et al. Mechanosensitive ion channels contribute to mechanically evoked rapid leaflet movement in Mimosa pudica. *Plant physiology*, 2021, vol. 187, no 3, p. 1704-1712.

[22] Barreto, Hayde Peregrina. "Segmentación de imágenes color aplicando los modelos de apariencia del color.",2018.

[23] Rueda Armelia, "Lo que no sabías de la "dormilona": mimosa púdica", 19 de mayo 2019. Leido por ultima vez el 1 de agosto 2022.

[24] Gutierrez Medina, Natalia Magaly, and Manuel Jesús Velazco Flores. Diseño y simulación de un sistema de detección de movimiento basado en segmentación de imágenes utilizando los métodos de umbralización y sustracción de fondo aplicado a un sistema de videovigilancia. 2019.

[25] Ieno, Egidio, et al. Simple generation of threshold for images binarization on FPGA. *Ingeniería e Investigación*, 2015, vol. 35, no 3, p. 69-75.

[26] Motta, Leonardo, et al. Automatic segmentation on thermograms in order to aid diagnosis and 2D modeling. *Proceedings of 10th workshop em Informática Médica*. 2010. p. 1610-1619.

[27] Asmaa Hosni, Michael Bleyer, Margrit Gelautz and & Christoph Rhemann, Local stereo matching using geodesic support weights, *Institute for Software Technology and Interactive Systems*, Vienna University of Technology Favoritenstr, (Viena, Austria), 2009, págs. 1- 2.G.

[28] Ethian, J. A. Level Set Methods and Fast Marching Methods: *Evolving Interfaces in Computational Geometry, Fluid Mechanics, Computer Vision, and Materials Science*, Cambridge University Press, 2nd Edition, 1999.

[29] De León-Martínez, José A.; Yañez-Ocampo, Gustavo; Wong-Villarreal, Arnoldo. Burkholderia species associated with legumes of Chiapas, Mexico, exhibit stress tolerance and growth in aromatic compounds. Revista Argentina de Microbiología, 2017, vol. 49, no 4, p. 394-401.

[30] García-Mateos, G., et al. "Segmentación automática de imágenes de cultivos: estudio comparativo de modelos de color." *Symposium Nacional de Ingeniería Hortícola*. 2014.

[31] Vaswani, Ashish, et al. "Attention is all you need." *Advances in neural information processing systems 30* (2017).